Chinese Chemical Letters 33 (2022) 1623–1626

Contents lists available at ScienceDirect

Chinese Chemical Letters

journal homepage: www.elsevier.com/locate/cclet

Metal-phenolic networks modified polyurethane as periosteum for bone regeneration

Qingyi Zhang[1], Kai Huang[1], Jie Tan, Xiongxin Lei, Liping Huang, Yuting Song, Qianjin Li, Chenyu Zou, Huiqi Xie*

Laboratory of Stem Cell and Tissue Engineering, Orthopedic Research Institute, Med-X Center for Materials, State Key Laboratory of Biotherapy, West China Hospital, Sichuan University, Chengdu 610041, China

ARTICLE INFO

Article history:
Received 27 June 2021
Revised 27 September 2021
Accepted 30 September 2021
Available online 4 October 2021

Keywords:
Metal-phenolic networks
Surface modification
Periosteum
Oxidative stress
Mineralization

ABSTRACT

Treatment of bone defects still poses a great challenge in orthopedic clinics, and the vital role of periosteum in such processes has attracted widespread attention. However, studies focusing on the oxidative stress micro-environment with an artificial periosteum at the site of defect have been scarce. The intrinsic anti-oxidative properties and therapeutic potential for bone defects of metal-phenolic networks (MPNs) have provided a potential solution to this. Herein, we have developed a protocatechualdehyde + zinc ion ($PCA+Zn^{II}$) MPN coating on a thermoplastic polyurethane membrane with a one-pot method to fabricate a new-type of periosteum with meritorious biocompatibility and abilities of modulating oxidative stress condition and promoting osteogenesis and mineralization for better bone regeneration, which has shown to be a promising strategy for constructing artificial periosteum with various MPNs.

© 2021 Published by Elsevier B.V. on behalf of Chinese Chemical Society and Institute of Materia Medica, Chinese Academy of Medical Sciences.

Bone defects, in particular those with an over critical size, remain as a major challenge in orthopedic clinics. Previous studies have mainly focused on the bone defects themselves, and therefore a diversity of transplanting strategies as well as tissue engineering bone grafts have been developed. However, delayed or even failed bone union still occurs in a considerable proportion of patients. As a matter of fact, the importance of periosteum, a "negligible" accessory of bones, has long been overlooked. During the last decade, growing evidences have suggested that the periosteum should be considered as a well-vascularized osteochondral organ which plays a significant role in the development and homeostasis of skeletal system as well as bone repair and reconstruction [1–3]. As estimated, the periosteum contributes to more than 70% of bone and cartilage formation at the early stage of autograft-mediated healing [4]. The healing effect of allografted bone may be largely limited due to devitalization or removal of the periosteum, whereas preservation or application of a periosteum graft may significantly enhance the bone reconstruction [5]. This has suggested a potential role of the periosteum in the treatment of critical-sized bone defects.

Various artificial periostea have been produced with biological and polymeric materials for preclinical and clinical usage [6–10]. Nevertheless, their primary purposes are still confined to serve as physical barriers to prevent soft tissue in-growth and scaffolds to support osteoblasts migrating to the defect area to promote bone regeneration, in addition to provide antibacterial property and signaling cues for osteoinduction [11,12]. So far, studies focusing on the oxidative stress micro-environment at the defect site have been scarce. Studies have demonstrated that oxidative stress can not only dramatically impair bone formation through inhibiting stem cell or progenitor cell viability and differentiation into osteoblast, but also provoke cell injury and apoptosis, both adversely affecting the quantity and quality of regenerated bone at the defect site [13–15]. Moreover, oxidative stress could simultaneously induce osteoclastogenesis and promote bone resorption, further aggravating the obstacles for bone reconstruction [16]. Under such contexts, to design and construct periosteum with excellent antioxidant stress property is a valuable strategy for bone regeneration.

Metal-phenolic networks (MPNs) are super-molecular networks assembled by the coordination drive of natural phenolic ligands and metal ions [17]. As the MPNs integrate the particular functions imparted by the phenolics molecules and metal ions, diverse functionalities may be customized through various combinations of the candidates, and to date thousands of MPNs-coated materials have been fabricated and applied for various fields [18]. In fact,

* Corresponding author at.
E-mail address: xiehuiqi@scu.edu.cn (H. Xie).
[1] These authors contributed equally to this work.

https://doi.org/10.1016/j.cclet.2021.09.105
1001-8417/© 2021 Published by Elsevier B.V. on behalf of Chinese Chemical Society and Institute of Materia Medica, Chinese Academy of Medical Sciences.

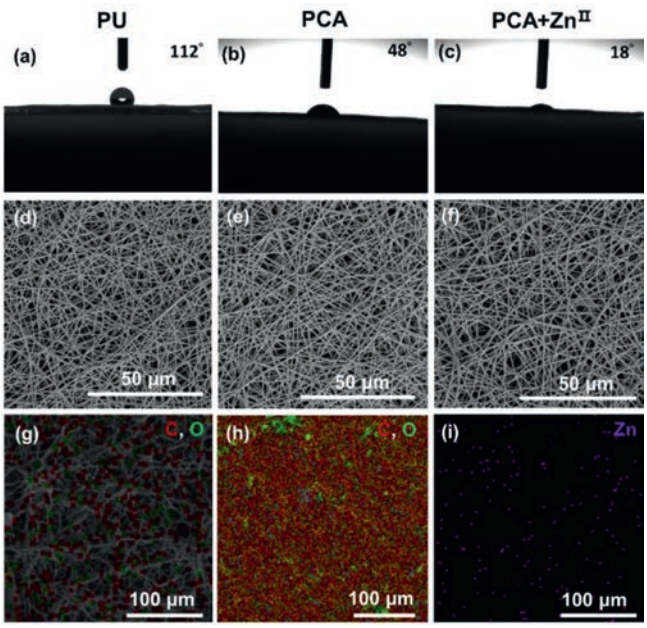

Fig. 1. (a-c) Water contact angle (WAC) images for water droplets on the surface of the PU group, PCA group and PCA+Zn^{II} group. (d-f) SEM images of the PU group, PCA group and PCA+Zn^{II} group along with (g-i) the EELS mapping analysis of each membrane.

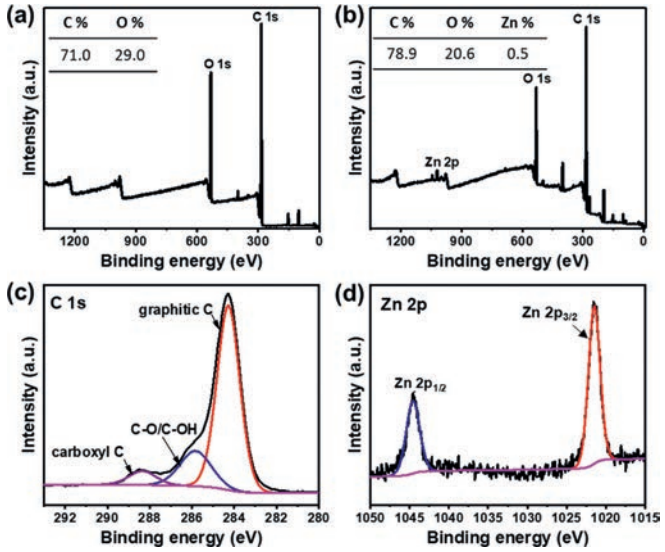

Fig. 2. XPS survey spectra and the content from XPS spectra (inset table) of the (a) PU group and (b) PCA+Zn^{II} group; (c) C 1s and (d) Zn 2p high-resolution spectra of the PCA+Zn^{II} group.

polyphenol itself, like protocatechualdehyde (PCA) for instance, has remarkable anti-oxidative properties, endowing with great potential in tackling oxidative stress [19–22]. As another candidate, certain metal ions such as zinc ion (Zn^{II}) may confer a beneficial effect with regard to the growth and mineralization of bone tissues through promoting cell proliferation and inducting matrix deposition [23,24]. Meanwhile, Zn^{II} can also inhibit osteoclastogenesis by regulating receptor activator of nuclear factor kappa-B ligand (RANKL) and subsequent RANKL/RANK/osteoprotegerin (OPG) axis [25]. Therefore, we assume that MPNs-coated artificial periosteum may introduce promising therapeutic effects.

To verify above hypothesis, PCA+Zn^{II} MPN coating on thermoplastic polyurethane (PU) membrane was designed in this study *via* simple one-pot deposition to fabricate an MPN-modified periosteum for bone regeneration (defined as PCA+Zn^{II} group). The pure PU membrane (PU group) and PCA coated PU membrane (PCA group) were used as control. This method was also extended to magnesium ion (Mg^{II}) and cupric ion (Cu^{II}) at the same time.

By analyzing the hydrophilicity of each type of membrane, we have found that, after coating treatment with PCA, the hydrophilicity of the PU membrane surface was significantly enhanced owning to the hydrophilic group from the phenolic building blocks [26,27]. Moreover, after PCA+Zn^{II} coating, the water contact angle (WCA) of the substrate surface was further reduced from 48° to 18° compared with the PCA group (Figs. 1a-c). Similar phenomena were also observed with the PCA+Mg^{II} and PCA+Cu^{II} coating, which indicated a great improvement of the hydrophilicity for the modified membranes (Figs. S1a and b in Supporting information). Of note, after the PCA+Mg^{II} coating, the WCA has reduced to 2°. The dramatic improvement may significantly enhance the repair of bone defects [28,29].

Scanning electron microscopy (SEM) has found no obvious aggregation, and the micropore structure of the PU membrane was preserved in the PCA and PCA+Zn^{II} groups (Figs. 1d-f) as well as the other two MPN groups (Figs. S1c and d in Supporting information). Meanwhile, the excellent uniformity and thin thickness of the coating has enabled the membrane in each group to retain the original functions of the substrate material such as filtration and size-matching devices.

Electron energy loss spectroscopy (EELS) mapping was carried out for each group (Figs. 1g-i). A uniform distribution of zinc element could be found on the surface of PCA+Zn^{II} groups. Meanwhile, energy dispersive X-ray (EDX)-elemental spectrum indicated a sound metal loading capacity of the MPNs coating (up to 1.3 wt%) and the ability to stabilize metal ions (Fig. S2a in Supporting information) [30,31]. EELS mapping results and EDX-elemental spectrum analysis of the other groups were also presented in Figs. S1e and f, and Figs. S2b-e (Supporting information), respectively.

Chemical bonding and element content analysis based on X-ray photoelectron spectroscopy (XPS) have determined the presence and content difference of C, O and Zn in the PCA+Zn^{II} group as compared to the PU group (Figs. 2a and b). Deconvolution of C 1s high-resolution spectra has disclosed the existence of C–O/C–OH (285.9 eV) and carboxyl C (288.5 eV) (Fig. 2c). Furthermore, the Zn 2p spectrum peaks at 1021.6 and 1044.8 eV were assigned to Zn^{II} in the adsorbent and may be attributed to Zn $2p_{3/2}$ and Zn $2p_{1/2}$, respectively (Fig. 2d). This suggested that Zn and PCA have successfully constructed the MPN by coordination. PCA and the other two metal ions (Mg^{II} and Cu^{II}) coated membranes were also measured *via* the XPS (Fig. S3 in Supporting information).

With respect to mechanical property, the stress-strain curves revealed that the mechanical properties were almost reserved after coating (Fig. S4a in Supporting information). Nevertheless, the elastic moduli have reduced from (38.9 ± 7.8) MPa to (20.5 ± 5.1) and (22.8 ± 2.5) MPa with the PCA and PCA+Zn^{II} coating, respectively (Fig. S4b in Supporting information). The three membranes have exhibited a tensile strength of (32.7 ± 1.0), (38.3 ± 6.6), and (38.2 ± 4.7) MPa, and their elongation-at-breaks was measured as (73.5 ± 7.1)%, (122.1 ± 12.4)% and (121.2 ± 9.3)%, respectively (Figs. S4c and d in Supporting information). These indicated that the coating in the PCA and PCA+Zn^{II} groups could even slightly improve the strength of the composites due to the hierarchical interaction (such as cation-π, hydrogen bond, catechol-metal coordination) between the coating and PU substrates [3,32,33]. Compared with the pristine PU group, both PCA and PCA+Zn^{II} groups showed promising mechanical strengths which may be beneficial for the construction of artificial periosteum.

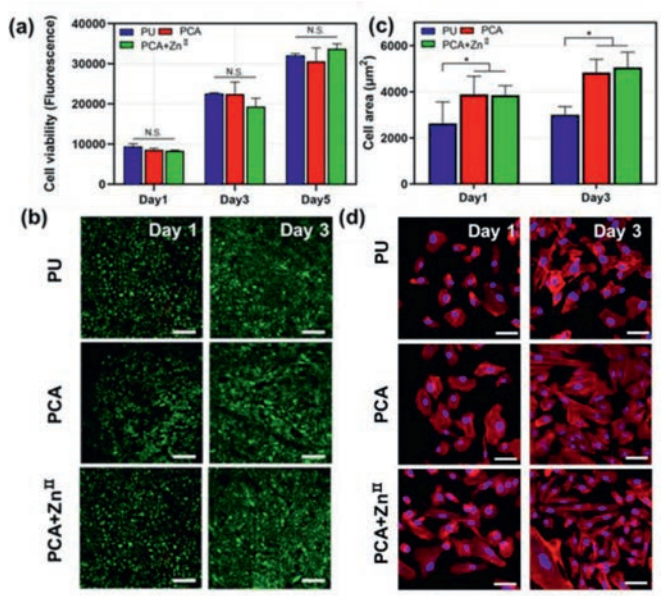

Fig. 3. (a and b) Cell proliferation and live/dead staining of the USCs on each membrane (scale bar = 500 μm). (c and d) Cell area and cytoskeleton staining of the USCs cultured on different membranes (scale bar = 15 μm). N.S.: non-significant, $^{*}P < 0.05$.

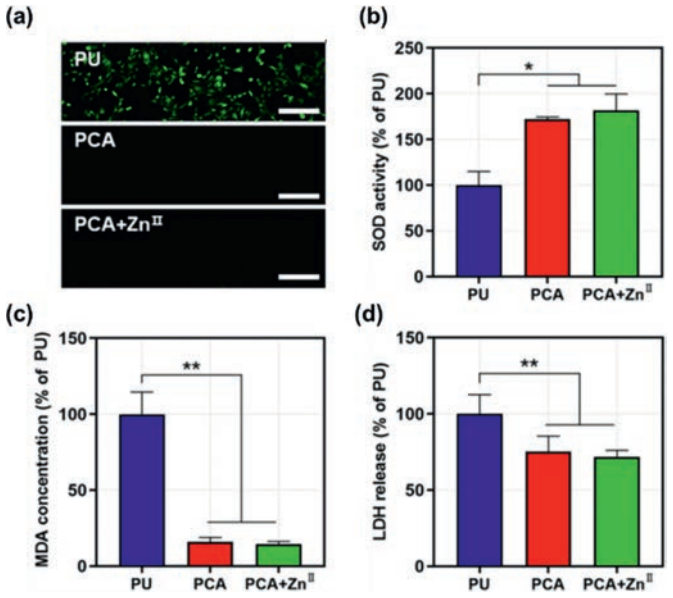

Fig. 4. (a) Intracellular ROS measured by DCFH-DA (scale bar = 500 μm). Measurement of the SOD activity (b) and MDA levels (c). (d) LDH release suggested cell damage under oxidative stress. $^{*}P < 0.05$, $^{**}P < 0.01$.

The proliferation of urine-derived stem cells (USCs) in the PU, PCA and PCA+Zn^{II} groups was quantified with alamar blue assay (Fig. 3a). The fluorescence intensity significantly increased in a time-dependent manner, and no differences in proliferation rate were detected after 1, 3 and 5 days of culture among three groups, which implied that the extra coating did not impair the original cytocompatibility. The living status of the USCs was also accessed by live/dead staining at 1 and 3 days, which indicated that the USCs proliferated well in each group, and dead cells were barely observed (Fig. 3b).

Imaging and quantitative analysis of cytoskeleton staining showed that USCs could adhere to the PU, PCA and PCA+Zn^{II} membranes. However, owning to the improved hydrophilicity after coating, superior spreading with a significant difference was observed in both the PCA and PCA+Zn^{II} groups after 1 and 3 days of culture. Accordingly, the cell area has remarkably increased in the PCA and PCA+Zn^{II} groups as compared with the PU group (Figs. 3c and d) [34,35]. By SEM, USCs displayed a spindle shape with thin filopodia in each group [36]. Cell proliferation and overlap could be clearly observed. Of note, both PCA and PCA+Zn^{II} groups performed better than the PU group in terms of the condition and morphology of the cells at all time points (Fig. S5 in Supporting information). Above results suggested that surface coating with PCA or PCA+Zn^{II} has conferred a superior spreading condition for the USCs.

The intracellular reactive oxygen species (ROS) level was measured with 2′,7′-dichlorofluoresceindiacetate (DCFH-DA) probe. After 24 h exposure to H_2O_2, ROS has notably accumulated in the cells seeded on the PU membrane as indicated by strong green fluorescence (Fig. 4a). By contrast, fluorescence signal was hardly detected when the USCs were cultured on both coated groups, suggesting that the PCA or PCA+Zn^{II} coating could effectively reduce intracellular ROS level. Above results have demonstrated an excellent ability of the MPN surface modification strategy for modulating the intracellular oxidative stress [37].

The oxidative status of each group was also evaluated. Following oxidative stimulation, the activity of superoxide dismutase (SOD) in the USCs seeded onto the PU was remarkably lower compared with those seeded onto the PCA or PCA+Zn^{II} membranes (Fig. 4b). Meanwhile, the final concentration of fatty acids peroxidation malondialdehyde (MDA) for the PCA and PCA+Zn^{II} coated membranes was also significantly decreased (Fig. 4c), suggesting that both have exhibited excellent anti-oxidative properties.

A lactic dehydrogenase (LDH) release assay was carried out to further analyze the cell damage in each group under the oxidative stress. In keeping with the results of SOD and MDA, the activity of extracellular LDH was significantly reduced in PCA and PCA+Zn^{II} groups, which suggested that the coated membrane could effectively alleviate cell damage after incubation with H_2O_2 (Fig. 4d) [38–40].

With respect to osteoinductive capability, as shown in Fig. 5a, the production of alkaline phosphatase (ALP) was remarkably enhanced on the PCA+Zn^{II} membrane after 1 and 3 weeks of osteogenesis culture as compared with the PU group and the PCA group. Intracellular ALP activity assay also revealed a significant difference between the PCA+Zn^{II} and PU group or PCA group after 1 and 3 weeks of culture (Fig. 5c), which suggested that the PCA+Zn^{II} membrane could induce the expression of ALP and promote the osteogenic differentiation. Of note, the ALP activity of the PCA group appeared to be lower than that of the PU group, which may be attributed to the influence of the PCA on the osteogenesis property of the USCs, albeit the difference was weak and without statistical significance.

Alizarin red staining (ARS) was carried out 2 and 3 weeks after the induction of osteogenesis. Similarly, calcium deposits were more obvious on the PCA+Zn^{II} membrane compared with the other two membranes (Fig. 5b). Accordingly in quantitative analysis, the content of extracellular sedimentary calcium in PCA+Zn^{II} group increased by 60.8% and 137.5% (Fig. 5d) after 2 and 3 weeks, respectively. The ARS results were in keeping with those of the ALP results, all indicating a promoted osteoinductive capability of the PCA+Zn^{II} coating.

In summary, we have designed and successfully synthesized a PCA+Zn^{II} MPN coating on the PU membrane by using a facile one-pot method to fabricate the artificial periosteum, which has shown a great potential for the treatment of bone defects. The physical and chemical properties as well as reaction mechanism of the PCA+Zn^{II} MPN have been evaluated in detail. The biocompati-

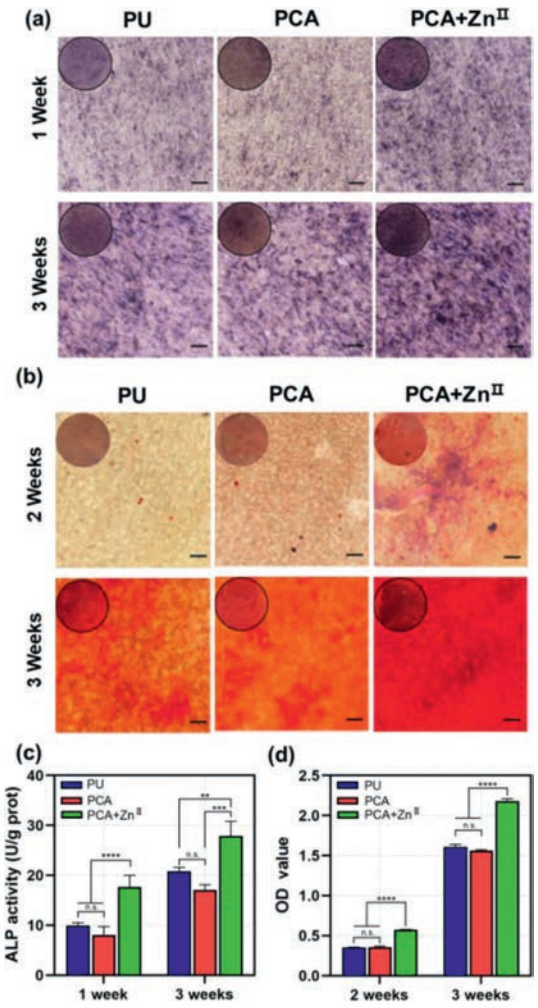

Fig. 5. (a and c) ALP staining and quantitative analysis of the PDLSCs after culturing in osteogenic medium for 1 and 3 weeks (scale bar = 100 μm). (b and d) ARS staining and quantitative analysis after 2 weeks and 3 weeks (scale bar = 100 μm). n.s.: non-significant, $^{**}P < 0.01$, $^{***}P < 0.001$, $^{****}P < 0.0001$.

bility and remarkable abilities of the MPNs in modulating oxidative stress micro-environment and inducing osteogenesis and mineralization as demonstrated in our study have shown a great promise to be further applied as periosteum materials for bone regeneration.

Declaration of competing interest

The authors declare that they have no known competing financial interests or personal relationships that could have appeared to influence the work reported in this paper.

Acknowledgment

This work was supported by the 1.3.5 Project for Disciplines of Excellence, West China Hospital, Sichuan University (No. ZYJC18002).

Supplementary materials

Supplementary material associated with this article can be found, in the online version, at doi:10.1016/j.cclet.2021.09.105.

References

[1] N. Li, J. Song, G. Zhu, et al., Biomater. Sci. 4 (2016) 1554–1561.
[2] J.G. Baldwin, F. Wagner, L.C. Martine, et al., Biomaterials 121 (2017) 193–204.
[3] L. Liu, C. Li, X. Liu, et al., ACS Biomater. Sci. Eng. 6 (2020) 4631–4643.
[4] X. Zhang, H.A. Awad, R.J. O'Keefe, R.E. Guldberg, E.M. Schwarz, Clin. Orthop. Relat. Res. 466 (2008) 1777–1787.
[5] T. Wang, Y. Zhai, M. Nuzzo, et al., Biomaterials 182 (2018) 279–288.
[6] L. Wu, Y. Gu, L. Liu, et al., Biomaterials 227 (2020) 119555.
[7] H. Li, H. Wang, J. Pan, et al., ACS Appl. Mater. Inter. 12 (2020) 36823–36836.
[8] R. Shi, M. Gong, C. Chi, et al., J. Biomed. Nanotechnol. 15 (2019) 272–287.
[9] R. Shi, J. Zhang, K. Niu, et al., Biomater. Sci. 9 (2021) 2090–2102.
[10] M. Gong, C. Huang, Y. Huang, et al., Nanomedicine 17 (2019) 124–136.
[11] G. Yang, H. Liu, Y. Cui, et al., Biomaterials 268 (2021) 120561.
[12] Q. Wang, J. Xu, H. Jin, et al., Chin. Chem. Lett. 28 (2017) 1801–1807.
[13] S.A. Sheweita, K.I. Khoshhal, Curr. Drug. Metab. 8 (2007) 519–525.
[14] S.K. Madhurakkat Perikamana, S.M. Lee, J. Lee, et al., Macromol. Biosci. 19 (2019) e1800392.
[15] M. Bacevic, B. Brkovic, A. Albert, et al., Calcified Tissue Int. 101 (2017) 553–563.
[16] Y. Hamada, H. Fujii, M. Fukagawa, Bone 45 (Suppl. 1) (2009) S35–S38.
[17] Z. Yang, W. Guo, P. Yang, et al., Polymer (Guildf) 221 (2021) 123627.
[18] H. Ejima, J.J. Richardson, F. Caruso, Nano Today 12 (2017) 136–148.
[19] S. Li, Y. Yu, J. Chen, et al., Molecules 21 (2016) 754.
[20] C. Guo, S. Wang, J. Duan, et al., Mol. Neurobiol. 54 (2017) 833–845.
[21] Z. Zhong, X. Yao, M. Luo, et al., Artif. Cell. Nanomed. B 48 (2020) 602–609.
[22] J. Qin, G. Liang, B. Feng, et al., Chin. Chem. Lett. 32 (2021) 842–848.
[23] H.J. Seo, Y.E. Cho, T. Kim, H.I. Shin, I.S. Kwun, Nutr. Res. Pract. 4 (2010) 356–361.
[24] H. Storrie, S.I. Stupp, Biomaterials 26 (2005) 5492–5499.
[25] C.J. Frederickson, J.Y. Koh, A.I. Bush, Nat. Rev. Neurosci. 6 (2005) 449–462.
[26] S. Pan, R. Guo, N. Bertleff-Zieschang, et al., Angew. Chem. Int. Ed. 59 (2020) 275–280.
[27] M.A. Rahim, S.L. Kristufek, S. Pan, J.J. Richardson, F. Caruso, Angew. Chem. Int. Ed. 58 (2019) 1904–1927.
[28] F. Rupp, L. Liang, J. Geis-Gerstorfer, L. Scheideler, F. Hüttig, Dent. Mater. 34 (2018) 40–57.
[29] R.S. Liddell, Z.M. Liu, V.C. Mendes, J.E. Davies, Clin. Oral Implan. Res. 31 (2020) 49–63.
[30] Q.Z. Zhong, S. Pan, M.A. Rahim, et al., ACS Appl. Mater. Inter. 10 (2018) 33721–33729.
[31] H. Geng, L. Zhuang, M. Li, et al., ACS Appl. Mater. Inter. 12 (2020) 29826–29834.
[32] A. Ho-Shui-Ling, J. Bolander, L.E. Rustom, et al., Biomaterials 180 (2018) 143–162.
[33] M. Gou, Y.Z. Huang, J.G. Hu, et al., ACS Biomater. Sci. Eng. 5 (2019) 5024–5035.
[34] Y. Zhang, L. Shen, Q.Z. Zhong, J. Li, Colloid. Surface. B 205 (2021) 111851.
[35] X. Xiong, X. Yang, H. Dai, et al., Stem Cell Res. Ther. 10 (2019) 396.
[36] P. Daugela, M. Pranskunas, G. Juodzbalys, et al., J. Tissue Eng. Regen. Med. 12 (2018) 1195–1208.
[37] S. Lee, J. Lee, H. Byun, et al., Acta Biomater. 124 (2021) 166–178.
[38] P. Ghensi, E. Bressan, C. Gardin, et al., Mat. Sci. Eng. C: Mater. 74 (2017) 389–398.
[39] X.T. Zhang, X.Q. Sun, C. Wu, et al., Biochem. Pharmacol. 148 (2018) 265–277.
[40] S.I. Voicu, R.M. Condruz, V. Mitran, et al., ACS Sustain. Chem. Eng. 4 (2016) 1765–1774.